

# Can catastrophic quenching be alleviated by separating shear and $\alpha$ effect?

Piyali Chatterjee, Axel Brandenburg and Gustavo Guerrero

(Received 00 Month 200x; in final form 00 Month 200x)

The small-scale magnetic helicity produced as a by-product of the large-scale dynamo is believed to play a major role in dynamo saturation. In a mean-field model the generation of small-scale magnetic helicity can be modelled by using the dynamical quenching formalism. Catastrophic quenching refers to a decrease of the saturation field strength with increasing Reynolds number. It has been suggested that catastrophic quenching only affects the region of non-zero helical turbulence (i.e. where the kinematic  $\alpha$  operates) and that it is possible to alleviate catastrophic quenching by separating the region of strong shear from the  $\alpha$  layer. We perform a systematic study of a simple axisymmetric two-layer  $\alpha\Omega$  dynamo in a spherical shell for Reynolds numbers in the range  $1 \leq R_m \leq 10^5$ . In the framework of dynamical quenching we show that this may not be the case, suggesting that magnetic helicity fluxes would be necessary.

*Keywords:* Dynamo, Magnetic helicity, Catastrophic quenching

## 1 Introduction

It is widely believed that the solar magnetic cycle is driven by an  $\alpha\Omega$  dynamo. The region of strong radial shear called the tachocline (Spiegel and Zahn 1992) at the bottom of the solar convection zone (SCZ) is believed to be the place where strong toroidal field is formed due to stretching of the weaker but diffuse poloidal field. It has been inferred from helioseismology that the tachocline is confined within a thin layer in the overshoot region which lies below the SCZ. This led Parker (1993) to propose the idea of an interface dynamo, where the shear is confined to a region with a greatly reduced turbulent diffusion, which also is the region of production of strong toroidal field. The helical turbulence generated due to convection and rotation in the layer above provides the turbulent  $\alpha$  and a large turbulent diffusivity  $\eta_t$ . The dynamo cycle being thus completed, the interface dynamo operates as a surface wave propagating along the boundary between strong shear and convection, which is also a region with a strong gradient in the turbulent diffusivity.

In order to mimic the process of dynamo saturation, traditionally authors have used an algebraic quenching function like  $\alpha_0/(1 + \overline{\mathbf{B}}^2/B_{\text{eq}}^2)$  or even  $\alpha_0/(1 + R_m \overline{\mathbf{B}}^2/B_{\text{eq}}^2)$ , where  $\alpha_0$  is the unquenched value of  $\alpha$ ,  $R_m$  is the magnetic Reynolds number,  $\overline{\mathbf{B}}$  is the mean magnetic field and  $B_{\text{eq}}$  is the equipartition magnetic field. However, it appears that conservation of magnetic helicity plays an important role in the process of saturation. At large  $R_m$ , the magnetic helicity ( $\int \mathbf{A} \cdot \mathbf{B} dV$ ) is fairly well conserved by the dynamo producing equal amounts of helicity in small and large scales, respectively. If the small-scale magnetic helicity is not able to escape out of the system, then the turbulent  $\alpha$  effect is markedly reduced (Pouquet *et al.* 1976). This leads to the magnetic energy of the dynamo to be quenched such that the saturation value varies as  $R_m^{-1}$ . Since astrophysical objects have large  $R_m$  ( $R_m \sim 10^9$  for the Sun), this strong dependence of the saturation field strength  $B_{\text{sat}}$  on  $R_m$  is referred to as *catastrophic quenching*.

Even though the helicity constraint in direct numerical simulations (DNS) of dynamos with strong shear has been clearly identified, the results can be matched with mean-field models having a weaker algebraic quenching of  $\alpha$  and turbulent diffusivity than  $\alpha^2$  dynamos (Brandenburg *et al.* 2001). However, the empirically determined coefficients would depend on circumstances and are therefore not universal. Such a model would not obey magnetic helicity evolution and is therefore untenable on theoretical grounds. The interface dynamo model has been invoked several times as a way of getting around the persistent problem of catastrophic quenching (see Charbonneau 2005, for a review). The belief is that the quenching function remains close to unity in the region of finite  $\alpha$  since the toroidal field is expected to be weak there. However, to our knowledge, this has never been verified in a consistent manner for a range of

magnetic Reynolds numbers. In this paper we perform a series of calculations with mean-field  $\alpha\Omega$  models, in spherical geometry, considering both algebraic and dynamical quenching formulations, for magnetic Reynolds numbers in the range  $1 \leq R_m \leq 2 \times 10^5$ . An important feature of these models is that the region of strong narrow shear is separated from the region of helical turbulence as proposed in the Parker's interface model.

In §2 we discuss the features of the  $\alpha\Omega$  model used, and the formulation of dynamical  $\alpha$  quenching. The results are highlighted in §3 and conclusions are drawn in §4. A part of the calculations presented in this paper will be discussed in a more detailed paper (Chatterjee *et al.* 2010). In this paper we focus specifically on the reality of the catastrophic quenching in dynamos with  $\alpha$  and  $\Omega$  effects operating in two widely separated layers.

## 2 Nonlinear $\alpha\Omega$ Dynamo

### 2.1 The underlying mean-field model

Our dynamo model consists of the induction equations for the toroidal component of the mean poloidal field potential,  $A_\phi(r, \theta)$ , and the mean toroidal magnetic field,  $B_\phi(r, \theta)$ , written in spherical geometry under the assumption of axisymmetry ( $\partial/\partial\phi = 0$ ). In some of the cases an additional evolution equation will be solved for the  $\alpha$  effect (described in the next section). We have used a modified version of the publicly available solar dynamo code *Surya*<sup>1</sup> described in Chatterjee *et al.* (2004) to perform these calculations.

In this paper we have used a smoothed step profile for  $\eta$  given by

$$\eta(r) = \eta_r + \frac{1}{2}\eta_t \left[ 1 + \operatorname{erf} \left( \frac{r - r_e}{d_e} \right) \right], \quad (1)$$

where  $r_e = 0.73R_\odot$  and  $d_e = 0.025R_\odot$ . We define the magnetic Reynolds number as  $R_m = \eta_t/\eta_r$ . In order to facilitate comparison with earlier work in Cartesian geometry (see, e.g., Brandenburg *et al.* 2009), it is convenient to define an effective minimal wavenumber,  $k_1$ . Somewhat arbitrarily, we use  $k_1 = 2/R_\odot$ , which corresponds to a harmonic wave with 2 nodes spanning the full latitudinal extent between both poles. We also define the wavenumber of the energy-carrying eddies,  $k_f$ , corresponding to the inverse pressure scale height near the base of the convection zone. For all our calculations we have taken  $k_f = 7k_1$ . Using the estimate  $\eta_t = u_{\text{rms}}/3k_f$  we can express the equipartition field strength with respect to the turbulent kinetic energy as

$$B_{\text{eq}} = (4\pi\rho)^{1/2}u_{\text{rms}} = (4\pi\rho)^{1/2}3\eta_t k_f.$$

For algebraic quenching there is no magnetic  $\alpha$  effect and we just have the kinetic  $\alpha$  effect,  $\alpha_K$ , which we assume to be of the form

$$\alpha_K(r) = \frac{1}{2}\alpha_0 \cos\theta \left[ 1 + \operatorname{erf} \left( \frac{r - r_a}{d_a} \right) \right] / \left( 1 + g_\alpha \bar{B}^2 / B_{\text{eq}}^2 \right), \quad (2)$$

where the value of  $\alpha_0$  may be computed using the first order smoothing approximation (FOSA) as being equal to  $\epsilon_f \eta_t k_f$  (Blackman and Brandenburg 2002). Here, the prefactor  $\epsilon_f$  is usually of order 0.1 or less since  $(\mathbf{u} \cdot \boldsymbol{\omega})_{\text{rms}} < u_{\text{rms}}\omega_{\text{rms}}$ . The case  $\epsilon_f = 1$  means the flow is maximally helical. The term  $g_\alpha$  is a non-dimensional coefficient equal to 1 or  $R_m$  depending on the assumed form of algebraic quenching in the models. Even though the helical turbulence pervades almost the entire convection zone, we take  $r_a = 0.77R_\odot$  and  $d_a = 0.015R_\odot$  so that we can have a large separation between the shear layer and the layer where turbulence is important. Consequently we consider a differential rotation profile like that in

<sup>1</sup>The code *Surya* and its manual can be obtained by writing an email to [arnab@physics.iisc.ernet.in](mailto:arnab@physics.iisc.ernet.in)

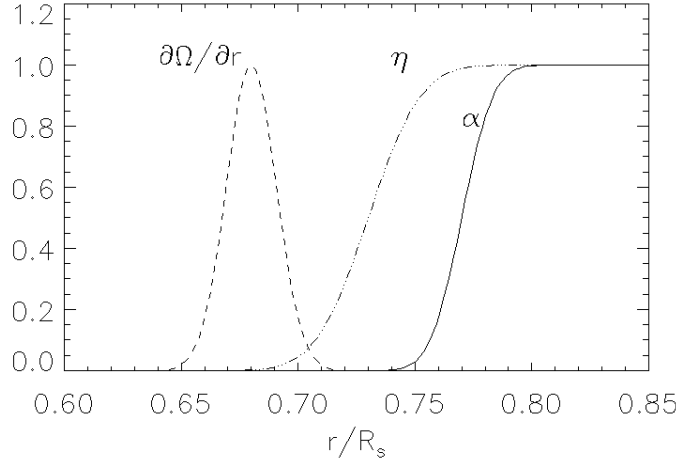


Figure 1. Profiles of negative radial shear  $\partial\Omega/\partial r$  (dashed),  $\alpha$  (solid) and  $\eta$  (dashed-dotted) as a function of fractional solar radius.

the high latitude tachocline of the Sun given by,

$$\Omega(r) = -\frac{1}{2}\Omega_0 \left[ 1 + \operatorname{erf} \left( \frac{r - r_w}{d_w} \right) \right], \quad (3)$$

where  $\Omega_0 = 14\text{nHz}$ ,  $r_w = 0.68R_\odot$  and  $d_w = 0.015R_\odot$ . The radial profiles of  $\eta_t$ ,  $\alpha$  and  $\partial\Omega/\partial r$  are plotted as a function of fractional radius  $r/R_\odot$  in Fig. 1. The region of strong radial shear is thus separated from the region of helical turbulence and the diffusivity has a strong gradient at a radius lying between the two layers. It may be noted that, in order to have supercritical dynamo action in a model with  $\eta$  having the same radial profile as  $\alpha$ , we must set  $\epsilon_f \gg 1$ . If the strong gradient of  $\eta$  lies between the two source regions, then we can work with  $\epsilon_f \leq 1$ . Also the time period  $T_{\text{cyl}}$  of the oscillatory dynamo remains a reasonably small fraction of the turbulent diffusion time  $t_{\text{diff}}$ . We can justify the profiles of  $\eta$  and  $\alpha$  on the grounds of having dynamo action for a reasonable range of parameters even while avoiding any significant overlap between the two source regions. The formulation of the equation for the evolution of the  $\alpha$  effect for dynamical quenching is described in §2.2.

## 2.2 Dynamical $\alpha$ quenching

It was first shown by Pouquet *et al.* (1976) that the turbulent  $\alpha$  effect is modified due to the generation of small-scale magnetic helicity such that the total  $\alpha$  effect is given by,

$$\alpha = \alpha_K + \alpha_M = -\frac{\tau}{3} (\overline{\boldsymbol{\omega} \cdot \mathbf{u}} - \rho^{-1} \overline{\mathbf{j} \cdot \mathbf{b}}), \quad (4)$$

where  $\boldsymbol{\omega}$ ,  $\mathbf{u}$ ,  $\mathbf{j}$ ,  $\mathbf{b}$  denote the fluctuating components of vorticity, velocity, current density, and magnetic field in the plasma, respectively.

For this type of quenching we use the same radial and latitudinal profiles of  $\alpha_K$  as given in Eq. (2), but without the algebraic quenching factor in the denominator, i.e. we put  $g_\alpha = 0$ . The second term in Eq. (4) is sometimes referred to as the magnetic  $\alpha$  effect or  $\alpha_M$ . It is possible to write an equation for the evolution of  $\alpha_M$  from the equation for the evolution of the small-scale magnetic helicity density  $h_f = \overline{\mathbf{a} \cdot \mathbf{b}}$  using the relation (Brandenburg *et al.* 2009),

$$\alpha_M = \frac{\eta_t k_f^2}{B_{\text{eq}}^2} h_f. \quad (5)$$

The equation for  $\overline{\mathbf{a} \cdot \mathbf{b}}$  is in principle gauge-dependent. However, under the assumption of scale separation, i.e. when the correlation length of the turbulence is small compared to the system size, one can define a magnetic helicity density of small-scale fields in a gauge-independent manner as the density of linkages Subramanian and Brandenburg (2006). Using Eq. (5), this leads to an evolution equation for  $\alpha_M$ ,

$$\frac{\partial \alpha_M}{\partial t} = -2\eta_t k_f^2 \left( \frac{\overline{\boldsymbol{\mathcal{E}} \cdot \overline{\mathbf{B}}}}{B_{\text{eq}}^2} + \frac{\alpha_M}{R_m} \right) - \nabla \cdot \mathbf{F}_\alpha, \quad (6)$$

where  $\overline{\boldsymbol{\mathcal{E}}}$  and  $\overline{\mathbf{B}}$  are the mean electromotive force and the mean magnetic field. The flux  $\mathbf{F}_\alpha$  consists of individual contributions, e.g., advection due to the mean flow, the Vishniac–Cho flux (Vishniac and Cho 2001, Subramanian and Brandenburg 2004), diffusive fluxes, triple correlation terms, etc. The effect of some of these individual fluxes in a spherical geometry and with both radial and latitudinal shear will be investigated in a paper under preparation (Guerrero *et al.* 2010), but for all the simulations presented in this paper we have put  $\mathbf{F}_\alpha = 0$ .

We solve the equations for  $A_\phi(r, \theta)$ ,  $B_\phi(r, \theta)$  and  $\alpha_M$  in a domain confined by  $0 \leq \theta \leq \pi$  and  $0.55R_\odot \leq r \leq R_\odot$ . The boundary conditions for  $A_\phi$  are given by a potential field condition at the surface (Dikpati and Choudhuri 1994) and  $A_\phi = 0$  at the poles. At the bottom we use the perfect conductor boundary condition  $\partial(rB_\theta)/\partial r = \partial(rB_\phi)/\partial r = 0$ . Also  $B_\phi = 0$  on all other boundaries. We have checked that the results are not very sensitive to different boundary conditions at the bottom boundary mainly because the boundary is far removed from the dynamo region. Since  $\mathbf{F}_\alpha = 0$ , no derivatives of  $\alpha_M$  need to be evaluated, so no boundary conditions need to be specified for  $\alpha_M$  and its evolution equation is just an initial value problem. We start with an initial dipolar solution where  $B_\phi$  is antisymmetric about the equator.

### 3 Results

To study the  $R_m$  dependence of  $B_{\text{sat}}$  in our model we keep all the dynamo parameters the same for all the runs except  $\eta_r$  which we change from  $2 \times 10^5 \text{ cm}^2 \text{ s}^{-1}$  to  $2 \times 10^{10} \text{ cm}^2 \text{ s}^{-1}$  while keeping  $\eta_t$  fixed at  $4 \times 10^{10} \text{ cm}^2 \text{ s}^{-1}$ . It may also be noted that the time period of the dynamo models ( $T_{\text{cyl}}$ ) is fairly independent of the magnetic Reynolds number.

To be able to correctly compare the dynamo models for different  $R_m$ , we have calculated the critical value of  $\alpha_0$ , denoted by  $\alpha_c$  for each model. In the following we present results for  $\alpha_0 = 2\alpha_c$ . We show in Fig. 2 the butterfly diagrams for  $B_\phi$  and  $\alpha_M$  at a depth of  $0.72R_\odot$ . It may be concluded from the butterfly diagram for  $\alpha_M$  in Fig. 2b that the small-scale current helicity, and hence  $\alpha_M$ , is predominantly negative (positive) in the Northern (Southern) hemisphere. Let us denote the exponential decay time for  $\alpha_M$  by  $t_\alpha$ . So,  $t_\alpha = R_m/\eta_t k_f^2 = 4.55 \times 10^{-3} R_m t_{\text{diff}}$ . For  $R_m = 2 \times 10^3$ , the decay time  $t_\alpha \gg T_{\text{cyl}}$  and so the system of equations is overdamped, as can be seen from the butterfly diagrams in Fig. 2a as well as from saturation curve (dashed dotted line) in Fig. 3. Note that there are amplitude modulations of the magnetic field before it settles to a final saturation value. The nature of the saturation curves of the magnetic energy is thus strongly governed by the ratio of  $t_\alpha$  and  $T_{\text{cyl}}$ .

The results of our calculations for different Reynolds numbers are plotted in Fig 3. The slopes in the kinematic phase are similar for all  $R_m$  within the error in the numerical determination of the critical  $\alpha_c$ . The strong  $R_m$  dependence, which is reminiscent of catastrophic quenching in large  $R_m$  dynamos, can be easily discerned from the same figure, but is more clear in Fig. 4 where we see that the saturation energy decreases monotonically as a function of magnetic Reynolds number. For  $R_m = 2 \times 10^5$ , the code has to be run for  $500 t_{\text{diff}}$  before the dynamo fields may start becoming ‘strong’ again for the case with  $\alpha_0 = 2\alpha_c$ . Due to long computational times involved in this exercise we have not continued the calculation beyond  $60 t_{\text{diff}}$ . Hence the determination of saturation magnetic energy may be inaccurate for  $R_m = 2 \times 10^5$ . In Fig. 4 we compare the case with dynamical quenching against the cases with a simple algebraic quenching of the form given in Eq. (2) with  $g_\alpha = 1$  and  $g_\alpha = R_m$ . We notice that for  $g_\alpha = R_m$ , the algebraically and dynamically quenched  $\alpha$  effects seem to give similar dependences on  $R_m$ .

When the code is run longer, we start seeing changes in the parity after  $t > 40 t_{\text{diff}}$  for the dynamically

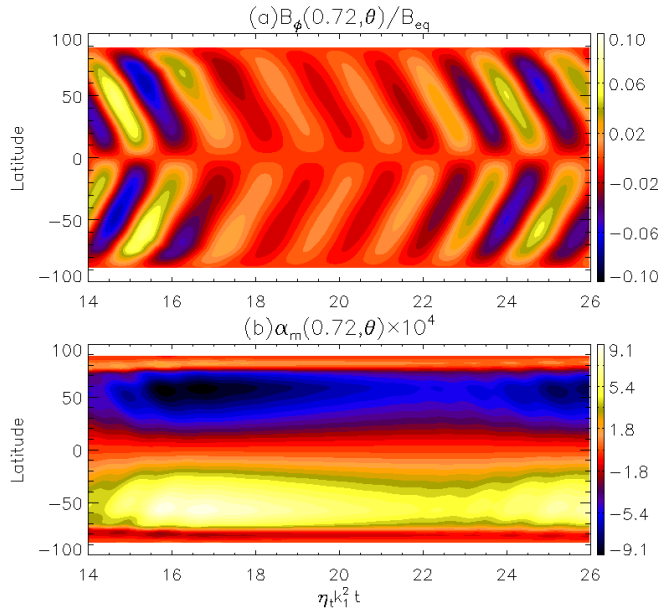


Figure 2. (a)  $B_\phi(0.72R_\odot, \theta)$  and (b)  $\alpha_m(0.72R_\odot, \theta)$  as a function of diffusion time  $\eta_t k_1^2 t$  for  $R_m = 2 \times 10^3$

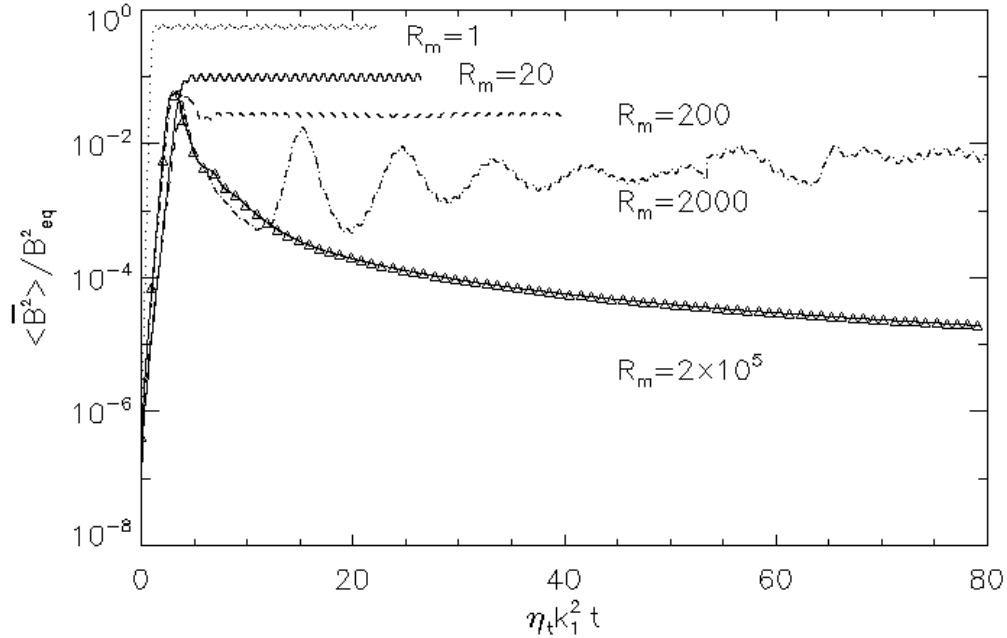


Figure 3. Volume averaged magnetic energy in the domain scaled with the equipartition energy for  $R_m = 1$  (dotted line),  $R_m = 20$  (solid),  $R_m = 200$  (dashed),  $R_m = 2 \times 10^3$  and  $R_m = 2 \times 10^5$  (triangles) with dynamical quenching. Adapted from Chatterjee *et al.* (2010).

quenched system in contrast to the strong' algebraic quenching case, where the parity remains dipolar. However the magnetic energy and the dynamo period  $T_{\text{cyl}}$  remain fairly constant even while the system fluctuates between symmetric and anti-symmetric parity at an irregular time interval.

In Fig. 5 we show the meridional snapshots in the Northern hemisphere of the toroidal component of the magnetic field and  $\alpha_M$ . It may be noted that the regions strongest in  $B_\phi$  become progressively confined in the narrow shear layer with increasing  $R_m$  while  $\alpha_M$  becomes stronger leading to decrease in  $B_{\text{sat}}$ . Even though  $\alpha_M$  is predominantly negative in the Northern hemisphere there is a region of positive small-scale helicity generated just below the region where  $\alpha_K$  is finite so that contribution from the term

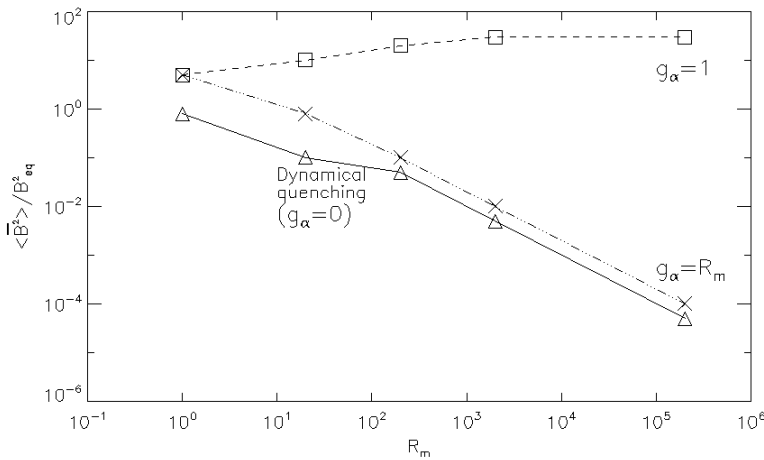


Figure 4. Volume averaged magnetic energy scaled with the equipartition energy in the saturation phase as a function of  $R_m$  for dynamical  $\alpha$  quenching (triangles +solid) and algebraic quenching with  $g_\alpha = 1$  (squares + dashed) and with  $g_\alpha = R_m$  (cross + dashed-dotted). Adapted from Chatterjee *et al.* (2010).

$\alpha B_\phi^2$  in the source  $\bar{\mathcal{E}} \cdot \bar{\mathbf{B}}$  is small. This effect is similar to the one reported in Brandenburg *et al.* (2009). We also have not observed any evidence of chaotic behaviour in the range of magnetic Reynolds number  $20 \leq R_m \leq 2 \times 10^5$  for twice supercritical  $\alpha$  ( $\alpha \leq 2\alpha_c$ ), in agreement with Covas *et al.* (1997)

#### 4 Conclusions

The calculations done in this paper indicate that it is not possible to escape catastrophic quenching due to accumulation of small-scale helicity in the domain by merely separating the regions of shear and  $\alpha$  effect. The saturation value of magnetic energy decreases as  $\sim R_m^{-1}$  for both dynamical quenching and the ‘strong’ ( $\sim R_m$ -dependent) form of algebraic quenching for the simple two-layer model. However, additionally we observe parity fluctuations for cases with dynamical quenching. It does not seem to us that there exists any chaotic behaviour in the time series of magnetic energy since the dynamo period and the saturation energy remains fairly constant. It may be possible that solar wind, coronal mass ejections, and Vishniac and Cho fluxes help in throwing out the small scale helicity from the Sun and thus alleviate catastrophic quenching. In this study we have not found any difference between the nature of the saturation curves for an  $\alpha\Omega$  dynamo and an  $\alpha^2$  dynamo using the form of dynamical quenching given by Eq. (6). However, it is clear that the algebraic quenching formula must fail if we were to allow for magnetic helicity fluxes that would, under suitable circumstances, alleviate catastrophic quenching.

We have been cautious about using dynamical quenching equation for dynamo numbers not very large compared to the critical dynamo numbers. We would expect that the magnetic field should affect all the turbulence coefficients including both  $\alpha$  and  $\eta$ . However for this analysis we have not included any quenching of  $\eta_t$ . This may be justified since such an effect could be mimicked by our simple two-layer model with a lower  $\eta_t$  in the region of production of strong toroidal fields and a higher  $\eta_t$  in the region of weaker poloidal fields. The effect of dynamical quenching on more realistic solar dynamo models having meridional circulation, Babcock-Leighton  $\alpha$  effect, and diffusive helicity fluxes have also been studied (Chatterjee *et al.* 2010).

Unfortunately the direct numerical simulations have not yet reached the modest Reynolds numbers used in this paper ( $\sim 10^4$ ) which are still much lower than the astrophysical dynamos. If  $B_{\text{sat}}^2$  really has an inverse dependence on  $R_m$ , then the solar dynamo should not be operating like it does! We may conclude that either we must have helicity fluxes out of the system or cross-equatorial diffusive fluxes inside the domain or that the  $\alpha_M$  equation to be used beside the mean-field induction equations must be suitably modified for  $\alpha\Omega$  dynamos. To verify if the equation for dynamical quenching works in the same way as in  $\alpha^2$  dynamos, we need to perform systematic comparisons between DNS with shear and convection and mean-field modelling for  $\alpha\Omega$  dynamos.

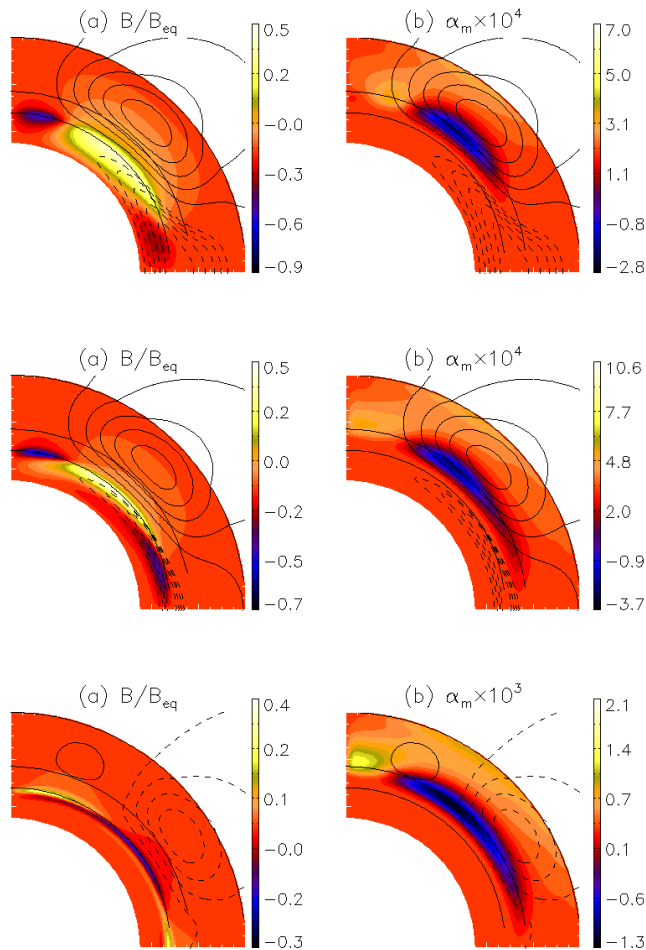


Figure 5. Meridional snapshots of (a)  $B_\phi/B_{\text{eq}}$  and (b)  $\alpha_m$  (color/grey-scale coded) for cases with different  $R_m$  starting from 20 (upper panel), 200 (middle panel) and  $2 \times 10^3$  (lower panel). Two concentric circles have been drawn at  $0.68R_\odot$  and  $0.77R_\odot$  to denote the radial positions of the shear layer and the  $\alpha$  effect. Solid and dashed lines denote poloidal field lines, corresponding to contours of positive (negative)  $r \sin \theta A_\phi$ .

### Acknowledgements

P.C. and A.B. would like to thank the organisers of the ‘Natural Dynamos’ meeting in High Tatras, where this work was initiated. We acknowledge the allocation of computing resources provided by the Swedish National Allocations Committee at the Center for Parallel Computers at the Royal Institute of Technology in Stockholm and the National Supercomputer Centers in Linköping as well as the Norwegian National Allocations Committee at the Bergen Center for Computational Science. This work was supported in part by the European Research Council under the AstroDyn Research Project No. 227952 and the Swedish Research Council Grant No. 621-2007-4064.

### REFERENCES

Blackman, E. G. and Brandenburg, A., “Dynamic nonlinearity in large scale dynamos with shear,” *Astrophys. J.* **579**, 359-373 (2002).  
 Brandenburg, A., Bigazzi, A. and Subramanian, K., “The helicity constraint in turbulent dynamos with shear,” *Monthly Notices Roy. Astron. Soc.* **325**, 685-692 (2001).  
 Brandenburg, A., Candelaresi, S. and Chatterjee, P., “Small-scale magnetic helicity losses from a mean-field dynamo,” *Monthly Notices Roy. Astron. Soc.* **398**, 1414-1422 (2009).

- Cattaneo, F. and Hughes, D.W., "Nonlinear saturation of the turbulent alpha effect," *Phys. Rev. E* **54**, R4532-R4535 (1996).
- Charbonneau, P., "Dynamo Models of the Solar Cycle," *Living Rev. Solar Phys.* **2**, 2 (2005).
- Chatterjee, P., Nandy, D., & Choudhuri, A. R., "Full-sphere simulations of a circulation-dominated solar dynamo: Exploring the parity issue," *Astron. Astrophys.* **427**, 1019-1030 (2004).
- Chatterjee, P., Guerrero, G. and Brandenburg, A., "Magnetic helicity fluxes in interface and flux transport dynamos," *Astron. Astrophys.*, submitted, arXiv:1005.5335 (2010).
- Covas, E., Tworkowski, A., Brandenburg, A. and Tavakol, R., "Dynamoes with different formulations of a dynamic  $\alpha$ -effect," *Astron. Astrophys.* **317**, 610-617 (1997).
- Dikpati, M. and Choudhuri, A. R., "The evolution of the Sun's poloidal field," *Astron. Astrophys.* **291**, 975-989 (1994).
- Guerrero, G. and de Gouveia Dal Pino, E. M., "How does the shape and thickness of the tachocline affect the distribution of the toroidal magnetic fields in the solar dynamo?" *Astron. Astrophys.* **485**, 267-349 (2008).
- Guerrero, G., Chatterjee, P. and Brandenburg, A., "Shear-driven and diffusive helicity fluxes in  $\alpha\Omega$  dynamos," *Monthly Notices Roy. Astron. Soc.*, submitted, arXiv:1005.4818 (2010).
- Jepps, S. A., "Numerical models of hydromagnetic dynamos," *J. Fluid Mech.* **67**, 625-646 (1975).
- Parker, E. N., "Hydromagnetic dynamo models," *Astrophys. J.* **122**, 293-314 (1955).
- Parker, E. N., "A solar dynamo surface wave at the interface between convection and nonuniform rotation," *Astrophys. J.* **408**, 707-719 (1993).
- Pouquet, A., Frisch, U. and Léorat, J., "Strong MHD helical turbulence and the nonlinear dynamo effect," *J. Fluid Mech.* **77**, 321-354 (1976).
- Subramanian, K. and Brandenburg, A., "Nonlinear current helicity fluxes in turbulent dynamos and alpha quenching," *Phys. Rev. Lett.* **93**, 205001 (2004).
- Subramanian, K. and Brandenburg, A., "Magnetic helicity density and its flux in weakly inhomogeneous turbulence," *Astrophys. J.* **648**, L71-L74 (2006).
- Spiegel, E. A. and Zahn, J.-P., "The solar tachocline," *Astron. Astrophys.* **265**, 106-114 (1992).
- Vishniac, E. T. and Cho, J., "Magnetic helicity conservation and astrophysical dynamos," *Astrophys. J.* **550**, 752-760 (2001).